Synthesis, Characterisation and Humidity Sensor Studies of Poly (Aniline-co-3-Trifluoromethyl Aniline) DBSA Doped Nanoparticles using Soft Template Polymerization

P S Vijayanand [1]*, S Jeeva [2], S Ashokan [3]

[1] Associate Professor, Department of Chemistry, Bannari Amman Institute of Technology, Erode, Sathyamangalam, Tamil Nadu, India

[2] Department of Chemistry, Bannari Amman Institute of Technology, Erode, Sathyamangalam, Tamil Nadu, India

[3] Department of Physics, Bannari Amman Institute of Technology, Erode, Sathyamangalam, Tamil Nadu, India

Email: [1] vijayanandps@bitsathy.ac.in

Abstract

Copolymers of aniline with 3-trifluoromethyl aniline functional polymers was synthesized using soft template polymerization. The surface morphology and crystalline nature of the materials are analysed using SEM, XRD analysis. The absorption bands around 320 and 620 nm in UV-vis spectrum indicate the presence of π-π* and n-π* transitions. SEM analysis represent the clustered or agglomerated spherical particles varying size from 100nm to 200nm. The amorphous nature of the polymers is confirmed by XRD pattern. The electrical nature of this materials ranges from 1.86×10^{-9} to 2.86×10^{-11} Scm^{-1} due to the steric effect of trifluoromethyl group. The relative humidity sensing characteristics was observed which is based on the resistance variations. This is due to the effective interaction of the water molecules with polymer matrix. The decreased in resistance is noticed 400 to 230 MΩ when the relative humidity (% RH) changes from 17 to 47%. Finally, this results clearly evidenced the functional polymers can be used in sensor industry.

Keywords: Functional poly aniline; copolymerization;3-trifluoromethyl aniline, FT-IR, SEM characterisation, humidity sensor.

1. Introduction

Nanostructured conducting polymers gains immense interest of research. In recent years, hence there is huge demand for the functional nanomaterials as electroactive nature in industrial area. Different nano-scaled morphological features of the functional polymers possess unique electrical properties. These polymeric materials act as a basic material for the manufacture of sensors, rechargeable batteries, solar cells and electromagnetic shield purposes. Hence polyaniline (PANI) based polymer is widely used for these applications because of structural, thermal stability and flexibility [1, 2], and widely used in the fabrications of all type of chemical and gas sensors, bio-technology and microelectronics field [3, 4]. The range of electro activeness in the conjugated macromolecules can be modified by means of controlled doping process, tuning the band gap structure in nano's

scaled architecture by means of templating method of synthesis in-order to make uniform ordered nanostructures [5-7]. Many synthesis methods have been taken to produce this material in lab scale to large scaled process such in-situ polymerization, physical blending and aqueous chemical oxidation method [8–10]. The poor solubility of the organic molecule occurs in various organic solvents in industrial processability [11-12].So in order to overcome this difficulty to enhance the better solubility characteristic various substituted aniline molecule are chosen because to bring improvements for change in polar characteristic by introducing the functional groups, as well as the electronic transport by anchoring the dopants inside without any kind of hindrance. Along with the conjugated pathway different type of charge carrier are also anchored to improve its electrical charecteristics with good film forming ability[13, 14]. The presence of side chain functional group in the molecular structures tends to changes the rigidity of the polymer chain [15]. Another type of chemical method to change the molecular environment is copolymerization process to improve the industrial film forming process, thus creating tailor-made materials by means of different arrangements of monomer sequences by means of random, block, and alternative orientation [16, 17]. To produce nanostructured materials several templating method are used such as several template oriented polymerization methods [18-23]. Among them micelle assisted anionic surfactant which forms micelle and can act as nanoreactor, structure directing agents[24]. Several inorganic nanomaterials are also added as a filler to polymer matrix to increase the charge transportation and also film stability are applied for biomedical and electronic industry [25-27].

In this research work we selected fluorine substituents monomers with aniline monomers for making copolymers. The covalent bond between carbon and fluorine group is responsible for high thermal stability and chemical resistance of the polymer. Since the C−F bond is low polarizable, the polymer has low moisture uptake and low dielectric constant [28].

The humidity sensors also play important roles as intelligent control systems for monitoring the environment. Most of the humidity sensor fails to detect the low content moisture in the atmosphere. Hence this work also focussed for the development of sensors. The low moisture sensing behaviour is very important factor in the fabrication of humidity sensors for tracking low quantity of moisture with better efficiency using polymer nanocomposites [29, 30]. Using aniline-co-m-trifluoromethyl aniline nanocomposites.

These nanostructured materials having higher surface area of different architecture which is beneficial in for designing the humidity and gas sensor [31-35].

The molecular structure and morphological features of the prepared nanostructured composites are thoroughly investigated.

2. Experimental Method

Aniline (Rankem, India) and 3-triflouromethyl aniline (Sigma-Aldrich, USA), Silver nitrate ($AgNO_3$), DBSA (Merck, India), ammonium persulfate $(NH_4)_2S_2O_8$ and concentrated hydrochloric acid were purchased from E-MERCK, India. Silver conducting paste purchased from Aldrich, USA.

2.1 Synthesis of Silver Nanoparticles

The silver nanoparticles were synthesized by the referring the procedure [36]. At first the predetermined amount of surfactant is taken distilled water and stirred for obtaining nanoreactor micelle, then aniline (0.184g) is take added and stirred gently to obtain clear solution, later AgNO3 solution of 0.019 M (0.339 g) is added gently. Further whole reaction mixture is stirred for 15 minutes by heating upto 90 degree Celsius. Finally, at first, 0.01 M (3.26 g) of DBSA was dissolved in 90 mL distilled water. Then 0.019 M (0.184 g) of aniline was added to the mixture, and stirred vigorously to form a transparent solution. $AgNO_3$ solution of 0.019 M (0.339 g) was added to the above solution dropwise to formed silver nanoparticles are obtained by centrifuging.

2.2 Synthesis of DBSA Doped Poly (Aniline-Co-3-Trifluoromethyl Aniline) Copolymer

In, 0.326 gm (0.01 M) of DBSA surfactant is taken 80 mL of distilled water. Then the mixture of 0.05 M (0.465 g) of aniline ,0.05 M (0.806 g) of3-trifluoromethyl aniline (3:3) is added slowly into the aqueous solution along with 10ml HCl solution. Finally, the oxidative initiator 10 mL of 0.1M (2.28 g) APS is injected into the solution for begin polymerization. The polymerization is continuing for 24 hours in an ice bath, the obtained dark green precipitate is filtered, washed and dried at at 40°C for about 6 hrs.The same procedure was repeated to for 3:2 and 3:1.

2.3 Characterization technique

ELICO SL-218 UV-Vis double beam spectrophotometer for analysing the bonding and non-bonding transitions. The symmetrical and asymmetrical stretching of the functional groups are recorded by ABB BOMEM B3000 FTIR range from 400–4000 cm^{-1}utilised for surface scanning aspects. Philips X'Pert Pro X-Ray diffractometer, with Nickel filtered CuKα radiation (λ = 1. 5402 Å) with the operation of 40 Kv for phase identification. The room temperature, conductivity was measured using a Keithley 6517B electrometer. The humidity sensor studies were measured using LCR-Q-meter 4910

3. Result and Discussion

3.1 Solubility

The solubility of three different copolymer composition samples was found to be completely soluble in polar solvents. About 0.5 mg of polymer sample and 5 ml of solvent are taken in a test tube and kept for 24 hoursat room temperature. The copolymer shows better solubility due to substituent groups in the polymer chain. These substituent groups reduce the stiffness of the polymer chain and increase the solvation property (Rao &Sathyanarayana 2003). The arrangement of dopant molecule and functional fluoro moiety changes the overall polarity of the molecules and improve its solvation properties (Lei&Su 2007). Solubility nature of the copolymers increases due to increase in comonomer feed (Ito et al 1998, Yin &Ruckenstein 2000, Laska&Widlarz 2003).

3.2 Absorption Analysis

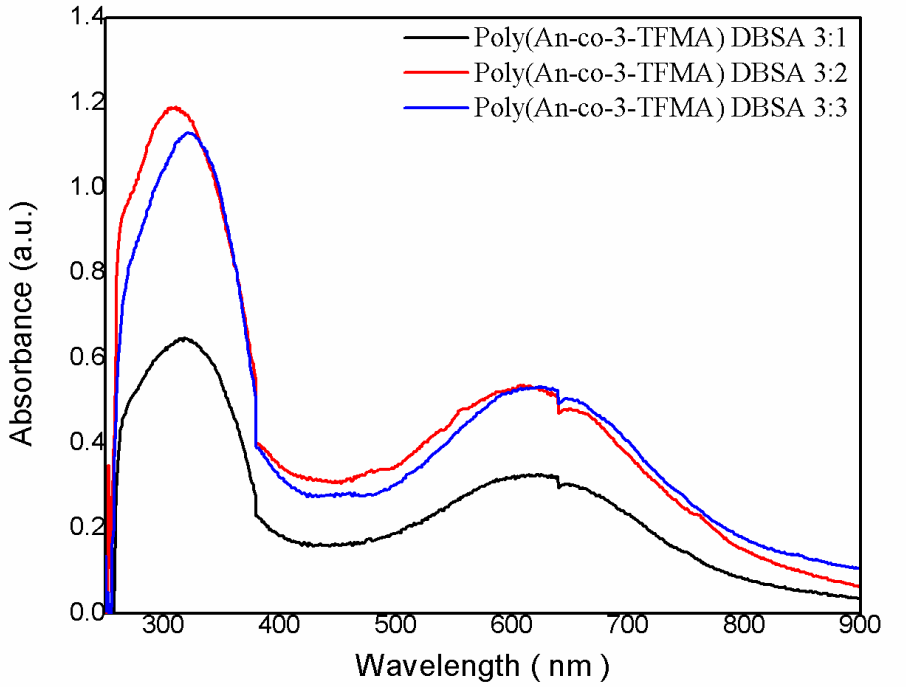

Figure 1 UV-Vis spectra of DBSA doped poly (An-co-3-TFMA)

Figure 1. illustrates the optical absorption spectra of DBSAdoped poly (An-co-3-TFMA) copolymer with various compositions ofmonomer and co-monomer feed ratio. The spectrum exhibits absorption band at 310 nm isdue to p-p* transitions of benzenoid ring and the absorption band at 620nm corresponds to n-p* transition of quinoid ring (Kim et al 1989, Gruger et al 1994, Lee & Cui 1996, Roe et al 1998). The 310 nm and 620nm peaks undergoes blue shift when the 3-TFMA concentration wasgradually increases. This blue shift is due to the alkyl substitution of 3TFMAin the polymer backbone. The polaronic peaks observed at 445,416 and 446 nm. It also evidenced for better solubility nature (Savitha et al 2005).

3.3 Functional Spectroscopy

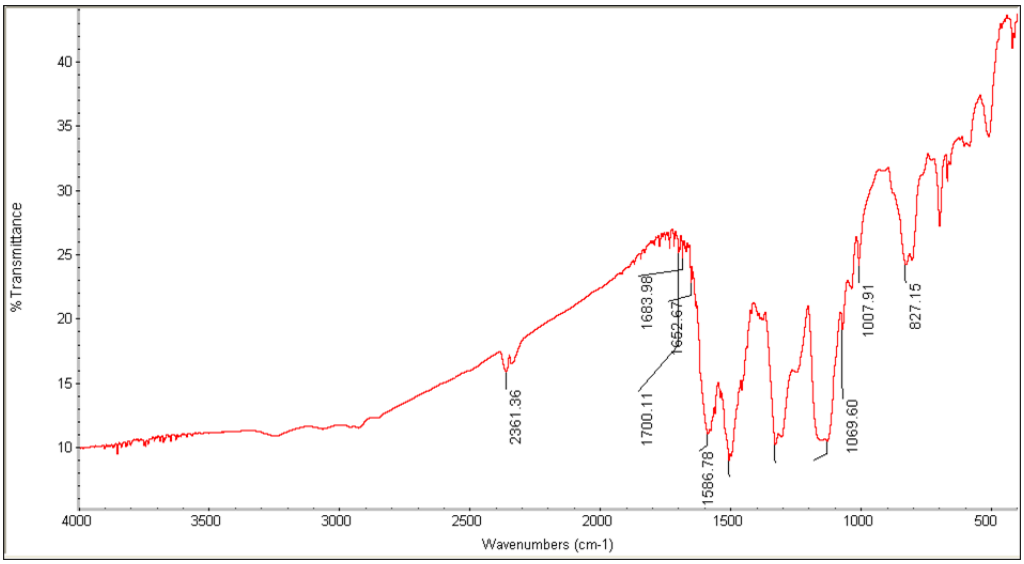

Figure 2 FT-IR spectra of DBSA doped poly (An-co-3-TFMA)

FT-IR spectra of DBSA doped poly (An-co-3-TFMA) copolymer shown (Figure 2) the DBSA doped poly (An-co-3-TFMA) copolymer nanoparticles. It shows characteristic bands at 3250, 3050, 2910, 1586, 1495, 1320, 1140,1007, 827 and 510 cm^{-1}. The band observed at 3250 cm^{-1} is attributed to the N-H stretching. The bands at 1582 and 1510 cm^{-1} respectively attribute to C=C and C=N stretching vibrations of benzenoid and quinoid rings. The characteristic bands at 3870, 3877, 3880 $cm^{-1}$and 2917,2925, 2926 cm^{-1} respectively correspond to symmetrical and asymmetrical stretching vibrations. The bands at 1733, 1734, 1739, 1740 cm^{-1} and 1582, 1587,1592 cm^{-1}relates to the C=C The bands at 1325, 1328,1335 cm^{-1}correspond to the N–H bending vibration and symmetric C=C stretching. The bands at 1165, 1166, 1171, and1128 cm^{-1}correspond to in-plane and out-of-plane–H bending vibration. The absorption band observed at 1028, 1030, 1040 cm^{-1}has been associated with the presence of halogen (fluoro) group in the copolymer. The bands around 1003, 1010, and1020 cm^{-1}correspond to the stretching vibration ofSO_3H^-. This characteristic peak confirms the presence of dopant as charge carriers into the polymer matrix.

3.4 Structural Analysis

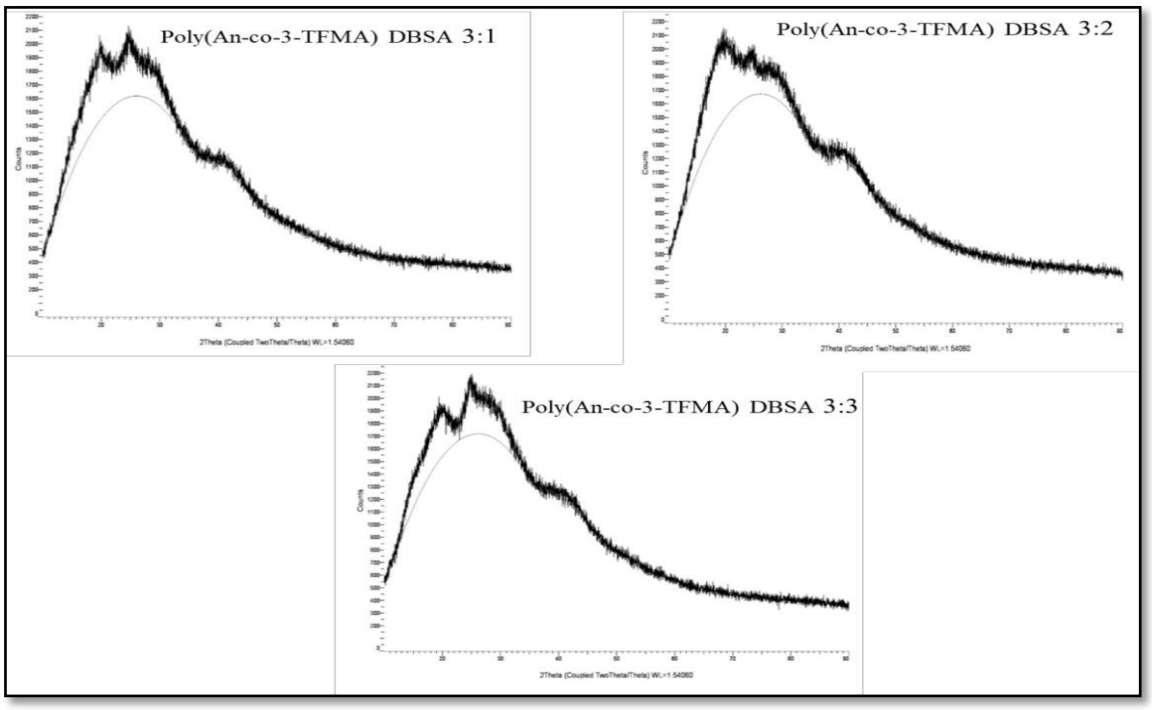

Figure 3. XRD pattern of DBSA doped poly (An-co-3-TFMA)

The XRD pattern of DBSA doped poly (An-co-3-TFMA) copolymer is shown in Figure 3. Two broad peaks observed at 18and25^o are shows the amorphous nature of the copolymer samples. This may be due to the irregular arrangement of polymer chains, attributed to the periodicity parallel and periodicity perpendicular to the polymer chain respectively (Biswas et al. 2014). The amorphous nature of the copolymer confirmed from these peaks. The broadening of the peak increases with increasing co-monomer concentration and results more amorphous nature. Further, the steric effect due to substituents does not allow them to crystallize.

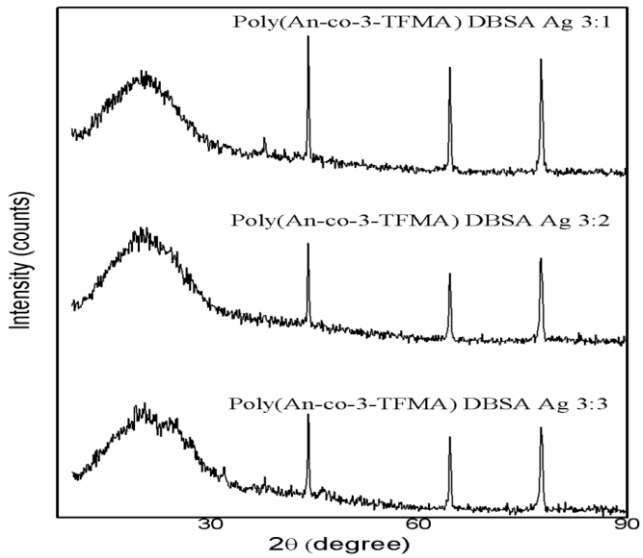

Figure 4. XRD pattern of Ag dispersed DBSA doped poly (An-co-3TFMA)

Figure 4. depicts the XRD pattern of Ag dispersed DBSA doped poly (An-co-m-TFMA) nanocomposites. It shows sharp peaks at2θ = 37.9, 44.1, 64.5and 77.3^{o} indicate the silver nanoparticles in the polymer matrix and were same with JCPDS no. 85-1355.

The silver dispersed copolymer exhibit more crystalline nature than the pure copolymer in absence of silver particles. For the DBSAdoped copolymer without thermal treatment exhibits the amorphous nature (Babazadeh 2009). This is attributed to the formation of copolymer inside the micelle, thereby controlling the particle size; and causes the amorphous nature rather to crystallise.

3.5 Morphological Studies

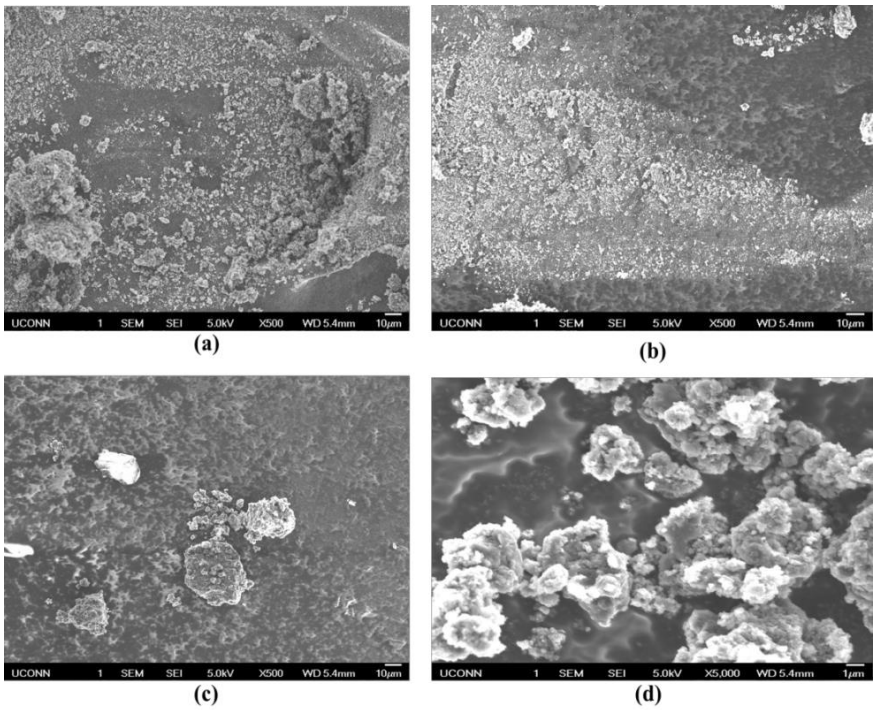

Figure 5. SEM image of DBSA doped poly (An-co-3-TFMA) (3:3)

Figures 5 (a-d) represents the surface morphology of DBSA doped poly (An-co-3-TFMA) copolymer. They exhibit highly agglomerated granular morphology appearance of the copolymer. It also exhibits the particle size of 100-200 nm. The surfactant molecule is responsible for granular and spherical morphology (Wan 2008). The formation of spherical shaped particles is due to the shape of surfactant micelle. Once after the formation of micelle, the polymerization takes place on to the core of micelle, the polymer chain starts to deposit on to the wall surface of the reactor as a microscopic nature. Due to the continuous polymerisation chain reaction, the chain length get increases which causes coiling of the chains to increases the sizes, during this polymerisation process, the layered like structures are also appeared. Overall it resembles in spherical shapes particles with layered structures inside it. It can be visualised into individual particles of isolated nature and some places the combination of micelle occurs. Because of the combination mixed irregular shape of particles also appears, but uniform arrangement of particle nature with well-defined boundary has been observed. The copolymer formed between the aniline and TFMA may be random or alternating or block nature. It all depends on the reactivity of the monomer molecules while polymerisation process.

3.6 Electrical Studies

Table 1. Electrical Parameters

Copolymer and its molar ratios	Conductivity (S/cm)
Poly (An-co-3-TFMA) DBSA 3:1	1.81×10^{-4}
Poly (An-co-3-TFMA) DBSA 3:2	7.55×10^{-4}
Poly (An-co-3-TFMA) DBSA 3:3	2.57×10^{-5}
Poly (An-co-3-TFMA) DBSA Ag 3:1	1.87×10^{-9}
Poly (An-co-3-TFMA) DBSA Ag 3:2	2.14×10^{-11}
Poly (An-co-3-TFMA) DBSA Ag 3:3	2.39×10^{-11}

The electrical conductivity value of DBSA doped poly (An-co-3TFMFA) nanocomposites values are shown in Table 1. It shows the electrical conductivity is in the range of 10^{-4} S/cm. The electrical conductivity is due to the improved movement of charge carriers through hydrogen bonding between the polymer chains. This charge transfer is inhibited by steric effect of bulky dopant molecules and substituted fluorine atoms in the benzene ring of the polymer chain. It is observed that the electrical conductivity decreased with increasing concentration of co-monomer ratio in the feed. This may be due to the electronegative fluorine atom decreases the movement of electrons along the polymer chain. The poly (An-co-3-TFMFA) nanocomposites depicts the electrical conductivity in the range of 10^{-11} S/cm. Furthermore, the substitution in the polymer backbone hinders movement of electrons resulting decreased electrical conductivity.

It reduces the movement of charge carriers and weakens the conductivity of polymer [49]. The decrease in the conductivity is due to the loss of crystallinity and is confirmed by XRD analysis. (iii) The trifluoromethyl substituent electron withdrawing effect might influence the

energy band and distribution of the electrons along the polymer chains. (iv) Bulky fluoro substituent will prevent acid doping of the polymers due to the electrostatic repulsion and steric hindrance. However, due to the presence of trifluoromethyl group the thermal stability of the composites will be increased.

3.7 Fabrication of Humidity Sensor

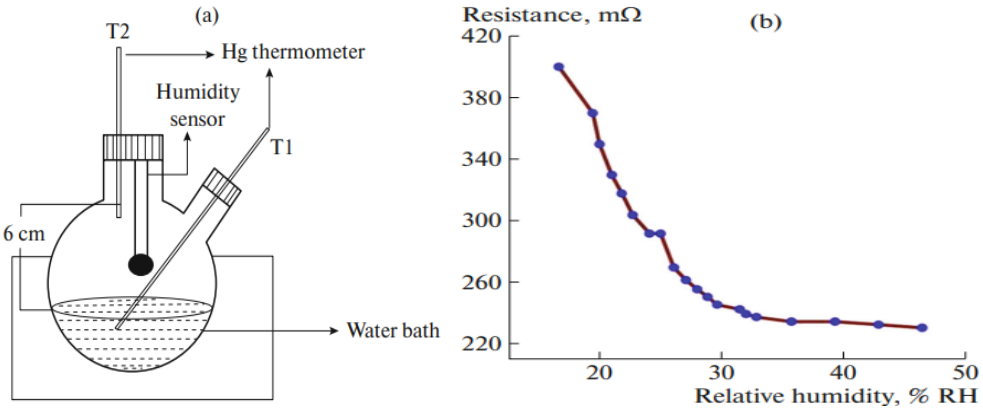

Figure 6. Humidity response (a) Experimental set-up (b) humidity sensing response

A thin film of the DBSA doped poly (An-co-mTFMA) copolymer was prepared by spin-coating method. About 100 mg of prepared copolymer was dissolved in 10 mL of DMSO. The solution was applied over the glass plate at 400 rpm and the film was dried. The thickness of the thin film was 30-70 μm [37]. Two copper wires were attached on the surface of the glass plate using a conducting silver paste. The prepared glass plate was placed inside a humidity chamber equipped with two-necked closed flask (250 mL) for placing thermometers and sensor. About 150 mL of distilled water was filled in the flask. The sensor plate and the thermometer were inserted through the one neck. Through the second neck of the flask another one thermometer was introduced to measure the temperature of the water inside the flask. Then the flask was placed in an ice bath. The temperature of the water was cooled to 15°C (T_2). The sensor plate was mounted 6 cm above from the water surface. To measure the temperature T_1 around the sensor plate, a thermometer was introduced at the same level of the sensor plate. The two terminals of the sensor plate were connected to a LCR meter to measure the changes in the resistance with respect to the temperature of the water from 15 to 25°C. The humidity inside the chamber was calculated by taking the ratio of the temperature of the water T_1 and temperature around the sensor plate T_2. The relative humidity (RH, %) inside the flask was calculated by the following Eq. (1) [38].

The humidity sensor was tested under different temperatures from 15 to 25°C in order to characterize the influence of temperature by recording the resistance variation of the sensor. Figure 5b shows humidity sensing response curve of copolymer. It clearly shows that at lower humidity atmosphere, the material possesses high resistance and the mobility of ions in the composite is restricted owing to curling up of polymer chain. At higher humidity environment it shows lower resistance character (consequently higher conductivity). The dopant molecules, the water molecules are weakly attached to the polymer by weak van der Waals forces of attraction. The water molecules adsorbed in the copolymer chain act as a source of proton for better electronic charge carrier.

The presence of spherical granules, inter granular or intra granular porosity as well as pore size distribution is also among the determinative factors for humidity sensing. The results revealed that the sensitivity of the sensor may decrease as the temperature increased, and the sensor had a high sensitivity at room temperature. It was studied at 30 and 75% RH separately. The sensor was shifted from 30 to 80% RH and the response time 55 s was noted. Figure 6 shows the long-term stability of DBSA-Ag doped poly(An-co-m-TFMA) composites. The conducting polymers, PANI and its derivatives have been found to be humidity sensitive for a long time.

4. Conclusion

A new series nanocomposites were synthesized by using chemical oxidative polymerization. The prepared samples characterized by various analysis. SEM results show that the composite film has spherical granular and nanolayered morphology. Electrical conductivity result shows the decrease in conductivity is due to decrease in conjugation and steric hindrance. XRD pattern shows the amorphous nature of copolymer. They have good chemical and physical properties different from those of the corresponding bulk material and homopolymer PANI. Thus, an effort has been made towards the design, synthesizing and characterizing of this new nanostructured conducting polymers. The prepared copolymer shows excellent humidity sensing response.

5. Acknowledgments

The authors gratefully acknowledge Ramakrishna Mission Vidyalaya College of Arts and Science for conducting the electrical conductivity studies.

References

[1] P. S. Rao and D. N. Sathyanarayana, Polymer 43, 5051 (2002).
[2] D. D. Borole, U. R. Kapadi, P. P. Mahulikar, and D. G. Hundiwale, Mater. Lett. 60, 2447 (2006).
[3] J. Stejskal, I. Sapurnia, and M. Trchová, Prog. Polym. Sci. 35, 1420 (2010).
[4] C. Della Pina, E. Falletta, and M. Rossi, Catal. Today 160, 11 (2011).
[5] J. J. Langer and K. Langer, Rev. Adv. Mater. Sci. 10, 434 (2005).
[6] K. Gupta, P. C. Jana, and A. K. Meikap, Synth. Met. 160, 1566 (2010).
[7] X. Feng, Y. Liu, C. Lu, W. Hou, and J. Zhu, Nanotechnology 17, 3578 (2006).
[8] H. H. Zhou, X. H. Ning, S. L. Li, J. H. Chen, and Y. F. Kuang, Thin Solid Films 510, 164 (2006).
[9] S. H. Jang, M. G. Han, and S. S. Im, Synth. Met. 110, 17 (2000).
[10] P. S. Vijayanand, J. Vivekanandan, A. Mahudeswaran, G. Ravikumar, and R. Anandarasu, Des. Monomers Polym. 18, 12 (2015).
[11] M. S. Cho, S. Y. Park, and J. Y. Hwang, Mater. Sci. Eng. C 24, 15 (2004).
[12] K. R. Reddy, K. P. Lee, and Y. Leel, Mater. Lett. 62, 1815 (2008).
[13] M. Babazadeh, Iran. Polym. J. 16, 389 (2007). 14. M. G. Han, S. K. Cho, S. G. Oh, and S. S. Im, Synth. Met. 126, 53 (2002).
[14] P. S. Rao, S. Subrahmanya, D. N. Sathyanarayana, Synth. Met. 139, 397 (2003).
[15] I. Willner, B. Willner, and E. Katz, Bioelectrochemistry 70, 2 (2007).
[16] H. He, J. Zhu, and N. J. Tao, J. Am. Chem. Soc. 123, 7730 (2001).

[17] C. Basavaraja, R. Pierson, and Do Sung Huh, Macromol. Res. 17, 609 (2009).
[18] X. Zhang and S. K. Manohar, Chem. Commun. 20, 2360 (2004).
[19] Y. Yan, Z. Yu, Y. W. Huang, X. W. Yuan, and Z. X. Wei, Adv Mater. 19, 3353 (2007)
[20] L. Haung, Z. Wang, H. Wang, X. Cheng, A. Mitra, and Y. Yan, J. Mater. Chem. 12, 388 (2002).
[21] Y. He and J. Lu, React. Funct. Polym. 67, 476 (2007). 23. Y. Ma, J. Zhang, G. Zhang, and H. He, J. Am. Chem. Soc. 126, 7097 (2004).
[22] W. Jia, E. Segal, D. Komemandel, Y. Lamhot, M. Narkis, and A. Siegmann, Synth. Met. 128, 115 (2002).
[23] W. L. Barnes, A. Dereux, and T. W. Ebbesen, Nature 424, 824 (2003). 26. R. C. Jin, Y. W. Cao, and C. A. Mirkin, Science 294, 1901 (2001).
[24] A. Choudhury, Sens. Actuators, B 138, 318 (2009).
[25] M. G. Dhara and S. Banerjee, Prog. Polym. Sci. 35, 1022 (2010).
[26] W. Luo, C. Cheng, and S. Zhou, Iran. Polym. J. 24, 573 (2015).
[27] Y. Sakai, Y. Sadaoka, and M. Matsuguchi, Sens. Actuators, B 35, 85 (1996).
[28] B. Adhikari and S. Majumdar, Prog. Polym. Sci. 29, 699 (2004).
[29] X.D. Cai, R. Huang, and Y. Guo, Chin. J. Polym. Sci. 31, 1443 (2013).
[30] C.-H. Lee, W.-Y. Chuang, S.-H. Lin, W.-J. Wu, and C.-T. Lin, Jpn. J. Appl. Phys. 52 (2013).
[31] Y. Ali, V. Kumar, A. S. Dhaliwal, and R. G. Sonkawade, Adv. Mater. Lett. 4, 368 (2013).
[32] Y. B. Wankhede, S. B. Kondawar, S. R. Thakare, and P. S. More, Adv. Mater. Lett. 4, 85 (2013).
[33] J. Yang, H. Yin, J. Jia, and Y. Wei, Langmuir 27, 5047 (2011). 37. P. S. Vijayanand, A. Jeeva, S. Ashokan, T. Kojima, S. Kato, and J. Chandrasekaran, J. Polym. Mater. 34, 637 (2017)
[34] S. Ashokan, V. Ponnuswamy, and P. Jayamurugan, South Asian J. Eng. Technol. 1, 11 (2015).
[35] W. Yin and E. Ruckenstein, Synth. Met. 108, 39 (2000).
[36] J. Laska and J. Widlarz, Synth. Met. 135, 261 (2003).
[37] G. Ravi Kumar, J. Vivekanandan, A. Mahudeswaran, and P. S. Vijayanand, Iran. Polym. J. 22, 923 (2013).
[38] P. K. Upadhyay and A. Ahmad, Anal. Bioanal. Electrochem. 1, 11 (2009).
[39] M. G. Roe, J. M. Ginder, and P. E. Wigen, Phys. Rev. Lett. 60, 2789 (1988).
[40] 44. A. Gruger, A. Novak, and A. Regis, J. Mol. Struct. 328, 153 (1994).
[41] P. S. Vijayanand, J. Vivekanandan, A. Jeeva, and R. ArunPrasath, Polym. Sci., Ser. B 58, 580 (2016).
[42] S. M. Reda and S. M. Al-Ghannam, Adv. Mater. Phys. Chem. 2, 75 (2012).
[43] S. Ding, H. Mao, and W. Zhang, J. Appl. Polym. Sci. 109, 2842 (2008).
[44] H. Swaruparani, S. Basavaraja, and C. Basavaraja, J. Appl. Polym. Sci. 117, 1350 (2010).

[45] K. C. Sajjan, S. Aashis, and A. Parveen, J. Mater. Sci.: Mater. Electron. 25, 1237 (2014).
[46] R. Singh, A. Yadav, and C. Gautam, J. Sens. Technol. 1, 116 (2011).
[47] W. D. Lin, H. M. Chang, and R. J. Wu, Sens. Actuators, B 181, 326 (2013).
[48] E. D. G1owacki, M. I. Vladu, and S. Bauer, J. Mater. Chem. B 1, 3742 (2013).
[49] A. T. Ramaprsad and V. Rao, Sens. Actuators, B 148, 117 (2010). 54. Q. Qi, T. Zhanga, S. Wanga, and X. Zheng, Sens. Actuators, B 137, 649 (2009).